

2001-03

Modeling the Contributions of the Exocytotic Machinery and Receptor Desensitization to Short- and Long-Term Plasticity of Synapses Between Neocortical Pyramidal Neurons

<https://hdl.handle.net/2144/2279>

"Downloaded from OpenBU. Boston University's institutional repository."

**Modeling the contributions of the exocytotic machinery
and receptor desensitization to short- and long-term
plasticity of synapses between neocortical pyramidal
neurons**

Murat Okatan and Michael Cohen

March, 2001

Technical Report CAS/CNS-01-003

Permission to copy without fee all or part of this material is granted provided that: 1. The copies are not made or distributed for direct commercial advantage; 2. the report title, author, document number, and release date appear, and notice is given that copying is by permission of the BOSTON UNIVERSITY CENTER FOR ADAPTIVE SYSTEMS AND DEPARTMENT OF COGNITIVE AND NEURAL SYSTEMS. To copy otherwise, or to republish, requires a fee and / or special permission.

Copyright © 2001

Boston University Center for Adaptive Systems and
Department of Cognitive and Neural Systems
677 Beacon Street
Boston, MA 02215

**Modeling the Contributions of the Exocytotic Machinery and
Receptor Desensitization to Short- and Long-term Plasticity of
Synapses between Neocortical Pyramidal Neurons**

Murat Okatan and Michael Cohen

April, 2001

Technical Report CAS/CNS-2001-003
Submitted to the Journal of Neuroscience

Department of Cognitive and Neural Systems and Center for Adaptive Systems
Boston University, 677 Beacon St, Boston, MA 02215
Phone: (617) 353-7858 or -7857, FAX: (617) 353-7755
E-mail: okatan@cns.bu.edu, mike@cns.bu.edu

Acknowledgments: MO was supported in part by the Defense Advanced Research Projects Agency and the Office of Naval Research (ONR N00014-95-1-0409) and the Office of Naval Research (ONR N00014-95-1-0657). We thank Daniel Bullock and Jen-Wei Lin for critically reading the manuscript and for helpful discussions.

Abstract

Short-term synaptic depression (STD) refers to the progressive decrease in synaptic efficacy during a spike train. This decrease may be explained in terms of presynaptic and postsynaptic processes, such as a decrease in the probability of transmitter release, and postsynaptic receptor desensitization. STD may be very strong, and is release-dependent in neocortical pyramid-pyramid synapses. Using a stochastic synapse model, we suggest that the main source of depression in these synapses is the step of vesicle priming, while vesicle depletion and postsynaptic receptor desensitization are proposed to play a lesser role. Our results suggest that vesicle priming may explain not only the release-dependent nature of STD, but also the observation that an average of about one vesicle per active zone is released in central synapses, without positing forced univesicular release. We propose that the latter phenomenon is due to a low priming probability. Our results also explain the effect of paired pre- and postsynaptic activity on STD. In neocortical pyramid-pyramid synapses pairing induces a form of long-term potentiation that has been described as a redistribution of synaptic efficacy (RSE). We propose that RSE is due to a pairing-induced increase in the probability that a primed vesicle will undergo release in response to a presynaptic action potential. This increase may be due to an increased Ca^{2+} influx through voltage-gated Ca^{2+} channels, or to an increased sensitivity of primed vesicles to this influx. The results were obtained by constraining the model with experimentally observed levels of release probability and other synaptic variables.

Key Words: Short-term depression, LTP, vesicle depletion, postsynaptic receptor desensitization, vesicle priming, univesicular release, multivesicular release, cortical pyramidal neurons, redistribution of synaptic efficacy.

Activity-dependent plasticity of chemical synapses is considered to be one of the main mechanisms by which the nervous system processes information and adapts itself to the environment. Understanding the rules that govern the mechanisms of synaptic plasticity is therefore expected to provide clues about the implementation of learning and memory within the nervous system. The present study aims at identifying and describing the synaptic mechanisms that underlie two widely studied forms of plasticity: short-term synaptic depression (STD) and long-term potentiation (LTP). The analysis that is presented is based on the data collected from single synaptic connections between tufted layer 5 pyramidal neurons (TL5 neurons) (Markram and Tsodyks, 1996; Tsodyks and Markram, 1997).

STD and LTP have been studied extensively in the past six decades in a wide variety of synapses and experimental conditions (Feng, 1941; Liley and North, 1953; Bliss and Lømo, 1973; Stevens and Wang, 1994; Stevens and Tsujimoto, 1995; Markram and Tsodyks, 1996; Tsodyks and Markram, 1997; Markram et al., 1998; Buonomano, 1999). It is known that potentiation (long-term or post-tetanic) affects the properties of STD in some synapses, including the pyramid-pyramid synapses in the neocortex (Ström, 1951; Liley and North, 1953; Eccles, 1957; Markram and Tsodyks, 1996; Tsodyks and Markram, 1997; Buonomano, 1999). Thus understanding the mechanisms that underlie STD may shed light on how LTP is expressed in these synapses.

STD may be due to several different synaptic mechanisms including the depletion of the vesicle pools (Liley and North, 1953; Stevens and Tsujimoto, 1995; Dobrunz and Stevens, 1997), postsynaptic receptor desensitization (Trussell and Fischbach, 1989; Colquhoun et al., 1992; Trussell et al., 1993; Jonas et al., 1994; Raman and Trussell, 1995; Jones and Westbrook, 1996; Otis et al. 1996; Angulo et al., 1997; Markram, 1997), calcium-induced inactivation of release machinery (Hsu et al., 1996; Bellingham and Walmsley, 1999), presynaptic inhibition through metabotropic glutamate receptors (mGluRs) (von Gersdorff et al., 1997), desensitization of presynaptic Ca^{2+} channels (Klein et al., 1980; Fox et al., 1987; Lemos and Nowycky, 1989; Cox and Dunlap, 1994; Forsythe et al., 1998; Patil et al., 1998; Wu et al., 1998), and the priming of vesicles for release (Bittner and Holz, 1992; von Rüden and Neher, 1993; Neher and Zucker, 1993; Chow et al., 1994; Heinemann et al., 1994; Südhof, 1995).

These mechanisms contribute to STD to different extents depending on the particular synapse and the experimental conditions that are being used. In the present study, the mechanisms that may significantly contribute to plasticity in TL5-TL5 synapses are identified first. Then, mathematical models are proposed for these mechanisms, which are ultimately combined to propose a stochastic synapse model. The model is then used to simulate STD data collected from TL5-TL5 synapses. Since data are available from these synapses both before and after the induction of LTP, the change in the model parameters may be used to determine the possible loci of synaptic plasticity involved in the expression of LTP.

MATERIALS AND METHODS

The Target Data. Markram and Tsodyks (1996) characterized STD in depressing excitatory synapses between tufted pyramidal neurons in somatosensory cortical layer 5 of the rat (named TL5 neurons in Markram, 1997). Their results are illustrated in Figure 1.

In this experiment they induced a presynaptic TL5 neuron to fire an action potential (AP) by injecting a 2 nA, 5 ms current pulse into its soma. They administered seven such injections spaced 43.48 ms apart (23 Hz) in each stimulus sweep. A new sweep was started every 5 s. The postsynaptic membrane potential trace (Post Vm) before pairing reflects the average of 58 sweeps and the one after pairing reflects the average of 59 sweeps in the same synaptic connection (Figure 1a). Resting membrane potential levels were -62 ± 2 mV.

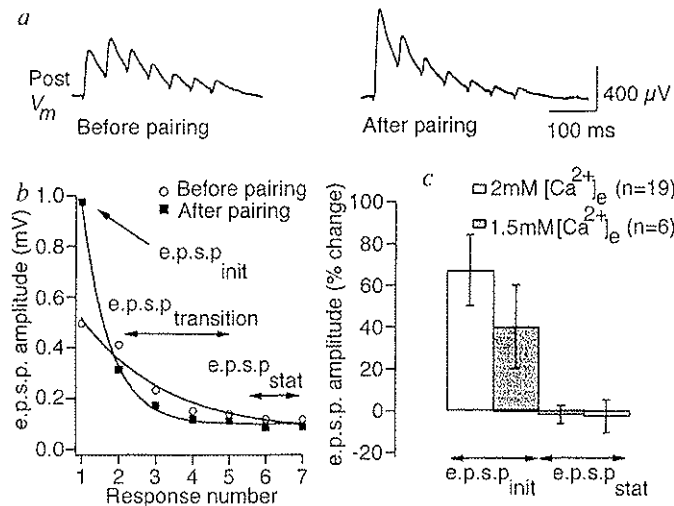


Figure 1. Short-term depression, and the effects of Hebbian pairing in cortical synapses. (a) Average membrane potential traces before (58 traces) and 20 min after pairing (59 traces). (b) EPSP amplitudes in (a) measured from the onset to the peak of an EPSP. STD manifests itself as a quick decrease in EPSP amplitude during stimulation. After pairing, the initial EPSP amplitude and the decay rate are larger, the amplitudes of the transition EPSPs are smaller, and no change is observed in the plateau EPSP amplitudes (EPSP_{stat}). Firing rate = 23 Hz. (c) Pairing-induced changes at two different concentrations of extracellular Ca^{2+} . No change is observed in EPSP_{stat} in either concentration level. (From Markram and Tsodyks, 1996)

The pairing method consisted of injecting sustained current pulses of 200 ms duration into visually identified individual presynaptic and postsynaptic TL5 neurons. The current intensity was adjusted to evoke 4–8 spikes and the current pulse in the postsynaptic neuron was delayed (1–5 ms) to ensure that the postsynaptic neuron discharged after onset of synaptic input. No attempt was made to control subsequent spikes. The procedure was repeated 30 times every 20 s.

The effect of paired-activity on EPSP amplitudes is illustrated in Figure 1b, where the EPSP amplitudes measured from Figure 1a are plotted. EPSP amplitudes were measured from the voltage immediately before the onset of the EPSP to the peak of the EPSP. Markram and Tsodyks (1996) described the effect of pairing as a redistribution of synaptic efficacy (RSE), which refers to the phenomenon that Hebbian pairing increases the average EPSP amplitude at the onset of a train, while the average amplitude of subsequent EPSPs may be increased, decreased or unaffected, indicating a redistribution of the synaptic efficacy in time (Figure 1b). They made the following observations about the results of the experiments.

1. The potentiation of the first response (Figure 1b) cannot be explained in terms of an increased absolute synaptic efficacy, since pairing did not affect the putative stationary EPSP amplitudes (see responses 6–7 in Figure 1b). Here the term absolute synaptic efficacy means the maximum amplitude of the postsynaptic response that can be elicited by an AP. It may be interpreted as a multiplicative synaptic gain, or weight.
2. The probability that an AP will fail to induce transmitter release (failure rate) decreased after pairing. Pairing decreased the failure rate from $21 \pm 5.4\%$ (before pairing) to $5 \pm 1.8\%$ (after pairing) in low extracellular Ca^{2+} concentration ($1.5 \text{ mM } [Ca^{2+}]_e$), and from $2.9 \pm 2.17\%$ to $0.33 \pm 0.25\%$ in high $[Ca^{2+}]_e$ (2 mM). Thus, pairing increased the release probability.
3. Pairing increased the rate of depression, and did not affect the rate of recovery from depression. Recovery time constant was $1,135 \pm 34 \text{ ms}$ before pairing and $1,133 \pm 51 \text{ ms}$ after pairing (11 synaptic connections).

4. The pairing-induced increase in the rate of STD was not caused by indirect effects of polysynaptic transmission as depression was not affected by the blockade of γ -amino butyric acid (GABA) receptors with picrotoxin (GABA-A) and saclofen (GABA-B).
5. The pairing-induced increase in the rate of STD was not caused by a change in metabotropic glutamate receptors (mGluRs) as depression was not affected by the blockade of mGluRs with 2-amino-5-phosphonopropionic acid.
6. Synaptic depression was not affected when postsynaptic voltage-activated channels were blocked after repatching and loading neurons with the lidocaine derivative, N-ethylbromide quaternary salt.
7. The fact that Hebbian pairing does not affect the stationary EPSP amplitudes (Figure 1b-c) indicates that the effect of pairing on these EPSPs can not be explained in terms of the recruitment or potentiation of postsynaptic receptors or unmasking of silent synapses in TL5-TL5 synapses.
8. The most likely mechanism for increased use of the existing synaptic efficacy is an increase in the probability of transmitter release after pairing.
9. RSE should be distinguished from unqualified potentiation or depression of synaptic efficacy, which imply a change in the gain of synaptic signals transmitted and which would be produced by mechanisms such as postsynaptic changes or by adding or removing synapses to or from the connection.

The present study proposes a stochastic synapse model that explains the properties of STD and LTP in these data while remaining consistent with the above observations. The model components are discussed next.

Depletion of the Releasable Vesicle Pool. Depletion of the vesicle pools has been used to explain STD in earlier studies (Liley and North, 1953; Grossberg, 1969; Betz, 1970; Zucker, 1989). According to these models, presynaptic stimulation results in vesicle exocytosis, which temporarily diminishes the number of vesicles in the releasable pool. This results in a decrease in the average number of vesicles released per presynaptic AP and hence a decrease in the average amplitude of the elicited postsynaptic response. Thus vesicle depletion contributes to STD. The releasable pool is refilled as vesicles migrate from the reserve pool to the releasable pool. This enables the releasable pool to be refilled during rest and therefore recovery from STD.

Anatomical evidence indeed shows that synapses do not contain a single homogeneous pool of vesicles. Two distinct pools of vesicles can be distinguished based on the presence of the protein synapsin (Greengard et al., 1993; Li et al., 1995; Pieribone et al., 1995; Shupliakov et al., 1996; Brodin et al., 1997). A two or three layer thick pool of vesicles adjacent to the active zone is devoid of synapsins (releasable pool), and a much larger distal pool of vesicles, continuous with the former pool, contains synapsins (reserve pool). The recovery from depression occurs with different time constants depending on the extent to which the pools are depleted (Liu and Tsien, 1995; Stevens and Tsujimoto, 1995).

In the experiments that are simulated here (Figure 1), test stimulations are not prolonged or intense enough to substantially deplete the reserve pool and the measured recovery time constants are assumed to reflect the time constant of the refilling of the releasable pool. The rate of refilling of the releasable pool is expected to be fast in the conditions under study. In studying the effects of cyclothiazide (CTZ) on STD, Markram (1997) observed that the recovery from STD occurred with a time constant of less than about 200 ms in TL5-TL5 synapses. CTZ is known to prevent the desensitization of postsynaptic α -amino-3-hydroxy-5-methyl-4-isoxazolepropionate (AMPA) receptors (AMPA receptors), and also has some presynaptic effects (Diamond and Jahr, 1995; Bellingham and Walmsley, 1999), but does not speed up the refilling of the releasable vesicle pool (Bellingham and Walmsley, 1999). Thus, the present study assumes that the arrival of a

vesicle at an empty release site may be modeled as a Poisson process with rate 200 ms in the target experiments.

The model of the depletion of the releasable vesicle pool is a modified form of the Katz model of transmitter release (Katz, 1969). The Katz model was originally proposed for the neuromuscular junction. According to a summary provided by Stevens (1993), in this model the neurotransmitter is released in discrete quantities of fixed size, called quanta, which are generally identified as the synaptic vesicles. When a nerve impulse arrives at a presynaptic terminal, calcium influx through voltage-gated calcium channels causes some vesicles to fuse with the axon terminal's surface membrane at special release sites called active zones and to release their contents into the synaptic cleft. Each active zone can release either zero or one quantum, and a neuromuscular junction has hundreds of active zones. Each quantum is released probabilistically and independently from the others, so that the number of released quanta, and hence the size of the response produced by the transmitter binding to postsynaptic receptors vary at random.

The Katz theory may be applied to central synapses after some modifications. The excitatory postsynaptic current (EPSC) amplitude elicited per excited active zone is variable in some central synapses. This variability may be due to the variability in such factors as the amount of transmitter released per vesicle, the relative positioning of the released vesicle and the postsynaptic receptors, and the occurrence of multivesicular release (Liu et al., 1999). It was proposed that the amount of transmitter that is released per active zone is variable even in the neuromuscular junction, despite the quantum hypothesis of the Katz theory (Kriebel and Gross, 1974; Wernig and Stirner, 1977). This variability was thought to arise from the release of more than one vesicles per active zone in the neuromuscular junction. Although the evidence for multivesicular release from the neuromuscular junction active zones is not strong (Magleby and Miller, 1981), this may be the mechanism that gives rise to the variability in the EPSC amplitude elicited per active zone in central synapses (Stevens, 1993). Recent evidence suggests that multivesicular release occurs in some central synapses, including the TL5-TL5 synapses (Auger et al., 1998). Thus, in this study, the Katz model is modified to allow for the release of more than one vesicle from a given active zone.

Accordingly, the present model implements the depletion of the releasable vesicle pool as follows. Each active zone is assumed to contain N release sites where a vesicle may be released. These release sites may correspond to the sites at which vesicles are morphologically docked in an active zone. In this study N is assumed to range from 1 to 25, similar to the number of docked vesicles observed in some hippocampal synapses (Schikorski and Stevens, 1997). Serial electron microscopic analysis suggests that a similar number of docked vesicles may be found in TL5-TL5 synapses (Markram et al., 1997). If the release is multivesicular, each of these sites may release a vesicle in response to a presynaptic AP, which for simplicity we assume is independent from the other sites. The release is probabilistic, in that if a vesicle is present at a release site at the time of an AP, it is released with the exocytotic probability $0 < u < 1$. u may vary during stimulation due to the priming of the vesicles. If the release is univesicular, then some vesicles are determined for release just like in the multivesicular mode, but only one of them is selected at random and released, while the release of the others is prevented for that round according to a winner-take-all scheme (Schikorski and Stevens, 1997). A site that is emptied by release refills a vesicle according to a Poisson process. The time constant of this process is assumed to be no larger than 200 ms during brief stimulations as in Figure 1.

A single synaptic connection between two TL5 neurons consists of 4 to 8 synaptic contacts (Markram et al., 1997). This number is denoted by the parameter C in the model. It is assumed that most of these contacts contain a single active zone (Markram et al., 1997). This is also consistent with the observation (Liu et al., 1999) that the great majority of synaptic boutons in hippocampal neurons also contain only one active zone, with estimates of the proportion ranging from 69% (Schikorski and Stevens, 1997) to 97% (Forti et al., 1997).

The values of the parameters C , N , and u may be constrained by the experimentally observed release probability of the synaptic connection where this information is available. For the data in Figure 1 information is available for the release probability at the first AP, both before and after pairing. The release probability from the synaptic connection at the first AP is given by the following equation:

$$\text{Pr} = 1 - (1 - u)^{NC}. \quad (1)$$

Here it is assumed that a vesicle is present at each release site at the first AP, as the synapse has fully recovered from STD at the beginning of each test stimulation. The number C of synaptic contacts per connection is important in determining the exocytotic probability and hence the extent of the depletion of the releasable vesicle pool during stimulation. Markram and Tsodyks (1996) reported that the release probability was $97.4 \pm 2.17\%$ before pairing, and $99.67 \pm 0.25\%$ after pairing in Figure 1 ($2 \text{ mM } [\text{Ca}^{2+}]_o$). Using Equation 1, the model parameters are constrained to yield a release probability in these ranges during the search for the optimal parameters that explain the data in Figure 1.

During simulations, the status of each release site is monitored individually. At the time of each AP, whether a vesicle is present at a site is determined. If a vesicle is not present, the site is refilled before the next AP with probability $1 - \alpha = 1 - \exp(-\Delta t / 0.2)$. Here Δt is the interspike interval, and 0.2 s is the Poisson rate of refilling mentioned above. If a vesicle is available, then it is selected for release with probability u . In multivesicular release mode all the selected vesicles are released. In univesicular release mode one of the selected vesicles is chosen at random and released, while the release of all the others is prevented for that round in that active zone. Although release sites in an active zone thereby interact in univesicular release, there is no interaction across synaptic contacts. Each synaptic contact behaves independent from the other contacts in both release modes.

Different sites in an active zone or in different contacts may have different exocytotic probabilities at a given time. The exocytotic probability of each release site is therefore monitored individually during simulations. Thus, the exocytotic probability of the release site "r" in contact "c" at the time of the n^{th} AP is denoted by the variable $u_{n,r,c}$. A schema representing the steps in the depletion and refilling of a given release site in multivesicular mode is shown in Figure 2. In univesicular mode the exocytotic probability may be smaller than $u_{n,r,c}$ due to the interaction between the sites selected for release.

The presynaptic transmitter output decreases during stimulation due to the depletion of the releasable vesicle pool. This affects the synaptic transmission to different extents depending on whether multivesicular release occurs and postsynaptic receptors are saturated by the transmitter content of a single vesicle. These issues are discussed next.

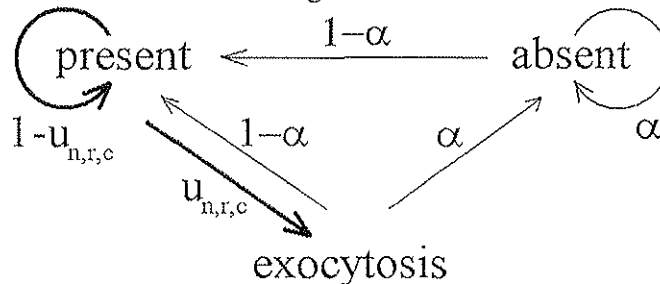


Figure 2. Depletion and refilling of a release site. The release site is in one of two states when an AP arrives: vesicle present or vesicle absent. Thick arrows represent instantaneous transitions induced by the AP. Thin arrows represent transitions that occur between APs. Shown next to each arrow is the associated transition probability. $\alpha = \exp(-\Delta t / 0.2)$, where Δt is the interspike interval and 0.2 s is the time constant of refilling of the release site. In univesicular release mode, the occurrence of exocytosis also depends on whether another release site in the same active zone has already started exocytosis. This interaction between release sites is not shown here, but is implemented in simulations as a winner-take-all procedure (Schikorski and Stevens, 1997). A site that is not permitted to release remains in the "vesicle present" state.

Saturation of Postsynaptic Receptors and Multivesicular Release. The release of further transmitter does not elicit significant incremental postsynaptic effects once postsynaptic receptors are saturated. The amount of transmitter that is sufficient for saturation is therefore a crucial parameter that determines the dynamic range of postsynaptic responsiveness to released transmitter.

The saturating amount of transmitter may be more or less than the transmitter content of a single vesicle. In large synapses, such as the calyceal synapses, the contents of single vesicles may not be sufficient for saturation (Trussell et al., 1993). In small synapses, such as hippocampal synapses, conflicting experimental results have been obtained about whether the transmitter content of a single vesicle can saturate postsynaptic receptors (Jonas et al., 1993; Tong and Jahr, 1994; Liu et al., 1999).

Theoretical approaches making use of AMPAR kinetics, and studies involving the application of short pulses of glutamate to out-side-out-patches suggested that the release of a single vesicle in central synapses may result in the occupation of at least 80% of postsynaptic AMPARs (Jonas et al., 1993; Tong and Jahr, 1994). These results suggested that doubling the transmitter concentration, as might occur in the synaptic cleft if two vesicles were released simultaneously, would have only a small effect on the peak amplitude of the current (Tong and Jahr, 1994).

A recent study by Liu et al. (1999) approached the problem with two different experimental strategies: One approach compared miniature EPSCs (mEPSCs) to currents evoked by localized application of glutamate at putative individual postsynaptic sites. The other strategy relied on molecular antagonism with a rapidly dissociating blocker of AMPA receptors. Their results suggested that glutamate receptors in hippocampal synapses are generally far from saturation during quantal transmission and that the variations in cleft concentration of glutamate may be the main cause of variability in EPSC size. The results of Liu et al. (1999) showed that quantal release is indeed not sufficient to saturate postsynaptic receptors in hippocampal synapses. As for the variability in EPSC amplitude, they pointed out that it may be due to such causes as the variability of the amount of transmitter released per vesicle, the variability in the relative positioning of the released vesicle and the postsynaptic receptors, and the occurrence of multivesicular release.

They also discussed the effectiveness of using kinetic models of AMPARs to reach conclusions about receptor occupancy. They noted that the models proposed so far may not have had adequate complexity to model AMPAR kinetics appropriately. Also, they emphasized the fact that the cleft concentration of glutamate may decay very fast after release due to lateral diffusion and binding to abundant glutamate transporters. This observation suggests that the fast glutamate application used by Tong and Jahr (1994), that maintained a glutamate concentration of 1 mM from a practically infinite reservoir for a period of 0.9 ms, might have constituted a stimulus that is much stronger than the release of a single vesicle. In other words, their glutamate pulse, which resulted in at least 80% receptor occupancy, might have been stronger than the transient increase in cleft concentration of glutamate that is due to the release of a single vesicle. Based on these results, the release of a single vesicle will not necessarily elicit a maximal postsynaptic activation in the stochastic model that is proposed here.

The non-saturation of postsynaptic receptors by the transmitter content of a single vesicle in a synapse is independent from whether multivesicular release occurs in that synapse. The existence of multivesicular release must be independently shown. Tong and Jahr (1994) provided evidence for the existence of multivesicular release in cultured hippocampal neurons using the competitive interaction between glutamate and N-methyl-D-aspartate (NMDA) receptor (NMDAR) antagonists. Multivesicular release was also shown to occur in inhibitory synapses that couple cerebellar inhibitory interneurons (stellate and basket cells) (Auger et al., 1998). Auger et al. (1998) stimulated single synapses with a single release site (active zone). They observed that the inhibitory postsynaptic current (IPSC) amplitude sometimes had a bimodal distribution, indicating that two or more

vesicles could sometimes be released per AP from the same active zone. Taking receptor occupancy into consideration, they proposed that the amplitude of an IPSC that would be elicited in response to the release of j vesicles would be given by:

$$I_j = I_1 \left(1 + (1 - \omega) + (1 - \omega)^2 + \dots + (1 - \omega)^{j-1} \right),$$

$$I_j = I_1 \frac{1 - (1 - \omega)^j}{\omega}, \quad (2)$$

where I_j is the IPSC amplitude, j is the number of vesicles that are released from the active zone, and $0 < \omega \leq 1$ is the receptor occupancy parameter.

Typical values of ω for TL5-TL5 synapses are not known. Auger et al. (1998) estimated the value of ω to be around 0.7 in synapses between cerebellar inhibitory interneurons. Similarly, ω is expected to be around 0.5 to 0.7 in excitatory synapses between hippocampal neurons in culture (Guosong Liu, personal communication, October 22, 2000). In the model, an intermediate value of 0.6 is used for ω .

Desensitization of Postsynaptic AMPARs. Postsynaptic glutamate receptors desensitize after exposure to glutamate and its agonists. Although both NMDA and AMPA receptors desensitize, NMDAR current is much smaller than that of AMPAR current at membrane potentials around -60 mV (Tong et al., 1995; Markram, 1997; Markram et al., 1997), which means that the postsynaptic component of STD is equivalent to AMPAR desensitization if the membrane potential fluctuates around -60 mV during STD. In the experiments associated with Figure 1 the membrane potential satisfied this condition (Markram and Tsodyks, 1996). It was shown that under similar conditions 95% of the EPSP amplitude was due to AMPAR current, while the rest was due to NMDAR current (Markram et al., 1997). Therefore, only the desensitization properties of AMPARs will be discussed in this article.

AMPA desensitization contributes to STD to different extents in different synapse types. Evidence from some brainstem and hippocampal synapses shows that the time constant of recovery from AMPAR desensitization is fast in these synapses (19 ms-Trussell et al., 1993; 48-58 ms-Colquhoun et al., 1992). Such small recovery time constants may suggest that AMPAR desensitization recovers to a large extent within one interspike interval at 23 Hz, which is the stimulation frequency in Figure 1. However, recovery from AMPAR desensitization occurs much slower in some other synapses, including the layer 5 pyramidal neurons. In these neurons, Jonas et al. (1994) measured that AMPAR current induced by a brief glutamate pulse recovers from desensitization according to a double-exponential process with a slow time constant of 767 ms. The magnitude $D(t)$ of the desensitization in units of the maximal response amplitude was given by:

$$D(t) = A_1 e^{-\frac{t}{\tau_1}} + A_2 e^{-\frac{t}{\tau_2}}, \quad (3)$$

where $A_1=0.18$, $A_2=0.3$, $\tau_1=56$ ms, and $\tau_2=767$ ms. Immediately after the first glutamate pulse, the amplitude of the response to a second pulse is only a fraction $1-D(0)=1-A_1-A_2$ of the amplitude of the response to the first pulse. The amplitude of the second response recovers according to Equation 3 as the interpulse interval t increases. This equation forms the basis of postsynaptic AMPAR desensitization in the present model.

The kinetics of desensitization and resensitization of AMPARs in layer 5 cortical pyramidal neurons can be described by the following equations:

$$S(t) = 1 - x(t) - y(t), \quad (4)$$

$$\frac{dx(t)}{dt} = \frac{-x(t)}{\tau_1} + A_1 S(t) R(t - t_n), \quad (5)$$

$$\frac{dy(t)}{dt} = \frac{-y(t)}{\tau_2} + A_2 S(t) R(t-t_n). \quad (6)$$

Here $S(t)$ represents the fraction of sensitive postsynaptic receptors while $x(t)$ and $y(t)$ represent the fast and slow components of desensitization, respectively. The function $R(t-t_n)$ is a Dirac's delta function $\delta(t-t_n)$ with a variable amplitude, and is triggered by release at the time t_n of the n^{th} AP in a test train:

$$R(t-t_n) = [1 - (1-\omega)^{\eta_n}] \delta(t-t_n). \quad (7)$$

The amplitude of $R(t)$ is determined by the number of vesicles that are released per active zone (Equation 2). Here ω represents the receptor occupancy, and η_n represents the number of vesicles that are released in response to the n^{th} AP.

As mentioned earlier, each synaptic contact acts independent of the other contacts in the model. Thus, the postsynaptic sensitivity level of each contact is monitored individually during the simulations. The postsynaptic sensitivity level is important in the calculation of the EPSP amplitude. Therefore only the value of the $S(t)$ at the time of an AP is used during computations. These values may be computed using difference equations instead of the differential Equations 4-6. These differential equations can be converted into the following difference equations:

$$S_{n,c} = 1 - x_{n,c} - y_{n,c}, \quad (8)$$

$$x_{n+1,c} = \left(x_{n,c} + A_1 S_{n,c} R_{n,c} \right) e^{-\frac{\Delta t}{\tau_1}}, \quad (9)$$

$$y_{n+1,c} = \left(y_{n,c} + A_2 S_{n,c} R_{n,c} \right) e^{-\frac{\Delta t}{\tau_2}}, \quad (10)$$

$$R_{n,c} = 1 - (1-\omega)^{\eta_{n,c}}, \quad (11)$$

$$\eta_{n,c} = \sum_{r=1}^N H_{n,r,c}, \quad (12)$$

$$H_{n,r,c} = \begin{cases} 1 & \text{if site } r \text{ of contact } c \text{ releases at the } n^{\text{th}} \text{ AP,} \\ 0 & \text{otherwise.} \end{cases} \quad (13)$$

Here Δt represents the interspike interval, which can be variable in irregular spike trains. The variable $H_{n,r,c}$ represents a binary flag that is 1 if the site r in contact c releases a vesicle in response to the n^{th} AP, and is 0 otherwise. This discretization leads to a tractable set of difference equations that are used in the search for the optimal model parameters.

Inactivation of Release Machinery and Vesicle Priming. Several processes intervene between the arrival of a vesicle to a release site and its release in response to an AP. This additional depression may be due to several processes that are downstream of the arrival of a vesicle to a release site. These processes include the docking of the vesicles, their being primed for release, and the operation of the release machinery that mediates vesicle fusion. Docking and priming consist of the formation of protein complexes that bind the vesicle to the presynaptic membrane in a manner that enables the dynamics of the protein complex to actuate the fusion of the vesicular and presynaptic membranes upon receipt of the exocytotic signal. This signal is the Ca^{2+} influx through presynaptic voltage-gated Ca^{2+} channels that are opened by a presynaptic AP (Söllner et al., 1993a, 1993b; Rothman, 1994; Scheller, 1995; Südhof, 1995; Benfenati et al., 1999).

It is commonly thought that an unprimed vesicle, namely a vesicle that is not bound to the presynaptic membrane by the appropriate protein complex (release machinery), may not be released in response to an AP. Part of this release machinery are one or more Ca^{2+} -sensing proteins that enable the release machinery to sense the presence of the exocytotic signal. The protein synaptotagmin is believed to be a major Ca^{2+} sensor of the release

machinery (Söllner et al., 1993a, 1993b; Scheller, 1995; Südhof, 1995; Shao et al., 1997; Geppert and Südhof, 1998), although evidence suggests that it is not the only Ca^{2+} sensor (Scheller, 1995; Benfenati et al., 1999; Elhamdani et al., 1999; Turner et al., 1999).

The competence of a vesicle for release is dependent on the formation of the release machinery complex and the sensitivity of that machinery to the exocytotic signal. It is conceivable that the disruption of all or part of the release machinery, or the inactivation of its Ca^{2+} sensors would result in the failure of the release machinery to mediate exocytosis in response to a presynaptic AP. In both cases, some aspect of the release machinery becomes temporarily inoperable due to some perturbation, and then it recovers with a finite rate. The affected aspect of the release machinery may be the very constitution of the protein complex, or the sensitivity of its Ca^{2+} -sensing protein. The perturbation may be the release of a vesicle (release-dependent case) or the presynaptic Ca^{2+} influx that may or may not result in release (release-independent case).

Inactivation of release machinery (IRM) was first described by Hsu et al. (1996) who also proposed a model for the state transitions of a putative Ca^{2+} sensor of the release machinery. A version of this model was used by Matveev and Wang (2000) in their synapse model (MW model) to explain the strong cortical STD observed in Figure 1. However, this explanation is not without some difficulties. First, IRM is proposed as a release-independent depression mechanism (Matveev and Wang, 2000). Namely, the presynaptic Ca^{2+} influx caused by an AP is thought to induce IRM even if no vesicle is released from the presynaptic terminal. It is known, however, that STD is release-dependent in pyramid-pyramid synapses in the neocortex (Thomson and Bannister, 1999). Second, recovery from IRM may occur too fast to explain the observed STD. In the experiments of Bellingham and Walmsley (1999), the process that was proposed to be the IRM recovered with a time constant of about 10 ms. These results suggest that IRM may not be the appropriate process to explain the strong STD observed in the target data.

While recovery from IRM may proceed too fast, vesicle priming, which is a process that proceeds with a much slower time constant, may be more appropriate in explaining the strong STD. Several biochemical processes intervene between the arrival of a vesicle to a release site and the exocytosis of that vesicle from that release site in response to an AP. These processes mediate the docking and priming of vesicles for release. It is commonly thought that a vesicle that arrives at a release site is first docked and then primed for fusion (Söllner, 1993a, 1993b; Rothman, 1994; Südhof, 1995; Benfenati et al., 1999). Of these two steps, docking proceeds faster, and is not a rate-limiting step during high-frequency stimulation (Südhof, 1995). Evidence suggests that priming occurs with a time constant on the order of a second (Chow et al., 1994; Heinemann et al., 1994).

The biochemical processes underlying docking and priming consist of the formation of a protein complex that binds the vesicular membrane to the presynaptic membrane. This complex includes SNAP receptor (SNARE) proteins that are attached to the vesicular membrane (v-SNARE) and the target presynaptic membrane (t-SNARE) (Söllner et al., 1993a, 1993b). Soluble NSF attachment proteins (SNAPs) are proteins that enable the *N*-ethylmaleimide-sensitive factor (NSF) to bind to the SNAREs. It was originally proposed that the v- and t-SNAREs formed a stable complex that attached the vesicle to the presynaptic membrane, and that the disruption of the SNARE complex resulted in the fusion of the vesicular and presynaptic membranes. The protein synaptotagmin was proposed to prevent this disruption in the absence of the exocytotic signal (Ca^{2+}). In response to the Ca^{2+} influx induced by the presynaptic AP, synaptotagmin would undergo a conformational change, and α -SNAP, which competes with synaptotagmin for its binding site on the SNARE complex, would replace the transformed synaptotagmin. Bound to the SNAREs, α -SNAP would then enable NSF to bind to the complex. In the presence of ATP, the binding of NSF has been proposed to disrupt the SNARE complex. This disruption was thought to energize the exocytotic fusion (Söllner et al., 1993a, 1993b; Rothman, 1994).

Recent results suggested that the above scheme may not be entirely correct. It is shown that the attachment of NSF to the SNARE complex occurs before fusion, during an ATP-dependent reversible step called priming, which follows docking but precedes Ca^{2+} -dependent fusion (Banerjee et al., 1996; Otto et al., 1997; Ungermann et al., 1998; He et al., 1999; Xu et al., 1999). Also, several other types of proteins have been discovered that have important roles in mediating exocytosis that are not accounted for by the above SNARE hypothesis (Südhof, 1995; Geppert et al., 1997; Benfenati et al., 1999; Jahn and Südhof, 1999; Lin and Scheller, 2000). In short, the individual steps of the biochemical processes that mediate docking, priming, and fusion of synaptic vesicles are yet to be completely identified. It is already known, however, that these protein interactions constitute a significant site of synaptic plasticity (Söllner, 1993a; Castillo et al., 1997; Doussau, 1998; Geppert and Südhof 1998; Turner et al., 1999; Lin and Scheller, 2000).

The fact that the vesicles need to be primed for fusion, and that this process proceeds with a time constant of the order of a few seconds after a vesicle arrives at the active zone, suggests that priming constitutes a refractory process downstream of the arrival of a vesicle at the active zone. Priming can be modeled as a two-state Markov process whereby a vesicle that has arrived at a release site is primed with a forward rate of $1/\tau^+$ and unprimed with a reverse rate of $1/\tau^-$ (Neher and Zucker, 1993; Heinemann et al., 1994; Banerjee, 1996; Xu et al., 1999; Matveev and Wang, 2000). Assuming that a vesicle arrives at a release site at time $t=0$, we have the following expression for the probability that it is in the primed state at time $t \geq 0$:

$$P_{\text{primed}}(t) = \frac{\tau^-}{\tau^- + \tau^+} \left(1 - e^{-\frac{t}{\tau}} \right) = \pi[1 - \gamma], \quad (14)$$

where $\tau = \tau^- \tau^+ / (\tau^- + \tau^+)$, $\pi = \tau^- / (\tau^- + \tau^+)$, and $\gamma = \exp(-t/\tau)$. Note that $P_{\text{primed}}(0) = 0$ since it is assumed that a newly arrived vesicle may not undergo fusion immediately and needs priming. This view of the mechanism of priming appears widely adopted, but some evidence suggests that at least some parts of the priming process may be completed even before docking (Ungermann et al., 1998; Lin and Scheller, 2000). At steady-state, $P_{\text{primed}} = \pi$.

In the case when a release site releases a vesicle at time $t=0$, the probability of finding a primed vesicle at that site at time $t \geq 0$ is given by:

$$Q_{\text{primed}}(t) = \pi \left[1 - \alpha - \frac{\tau}{\tau - \tau_{\text{refill}}} (\gamma - \alpha) \right] = \pi G, \quad (15)$$

where $\alpha = \exp(-t/\tau_{\text{refill}})$, and $\tau_{\text{refill}} = 0.2$ s is the Poisson rate of the arrival of a vesicle to the site, i.e. refilling rate. The expression in Equation 15 is the solution of the integral

equation $Q_{\text{primed}}(t) = \int_0^t \frac{1}{\tau_{\text{refill}}} P_{\text{primed}}(t-x) e^{-\frac{x}{\tau_{\text{refill}}}} dx$, where $P_{\text{primed}}(t-x)$ is used from Equation

14. This integral represents the summation of all probabilities of finding a primed vesicle at time $t \geq x \geq 0$ given the fact that a vesicle arrived at the site at time $x \geq 0$.

If a vesicle is found at the primed state at time $t=0$, and that vesicle is not released at time $t=0$, then the probability that the vesicle is in primed state at time $t \geq 0$ is given by:

$$T_{\text{primed}}(t) = \gamma + \pi[1 - \gamma] = \Phi, \quad (16)$$

which is computed as Equation 14, with the additional fact that $T_{\text{primed}}(0) = 1$, as learned from the observation of the priming state of the vesicle at $t=0$. Finally, if an existing vesicle is found at the unprimed state at time $t=0$, then the probability that the vesicle is in primed state at time $t \geq 0$ is given by Equation 14.

Different assumptions may be made about the role of priming in release. Here, a model that is based on the following assumptions is described.

In multivesicular mode:

If a vesicle is in primed state at the time of an AP, then it is selected with probability $0 < \epsilon \leq 1$ for release, and all of the selected vesicles are released.

In univesicular mode:

If a vesicle is in primed state at the time of an AP, then it is selected with probability $0 < \epsilon \leq 1$ for release, and one of the selected vesicles is chosen at random and is released. The others are not released for that round. The selected vesicles have equal probability of being chosen for release.

The above model of vesicle priming may be coupled with the models of depletion of the releasable vesicle pool, and AMPAR desensitization, to explain the target data. Before discussing an approximate model that captures the average behavior of the stochastic model, the next section discusses some other synaptic mechanisms that are known to contribute to STD, but that were not significant in the target experiments.

Other Synaptic Processes. In this section, two more presynaptic processes are introduced that have been shown to contribute to STD under certain circumstances and in some preparations: inhibition of transmitter release via presynaptic metabotropic glutamate receptors (mGluRs), and inactivation of presynaptic Ca^{2+} channels that mediate the AP-induced Ca^{2+} influx to the presynaptic terminal.

von Gersdorff et al. (1997) showed that the contribution of presynaptic mGluRs to synaptic depression is less than 10% in the frequency range from 5 Hz to 10 Hz in Calyx of Held synapses in the rat brainstem (21-25 °C). They also noted that this contribution would be even smaller at physiological temperatures, since glutamate uptake is faster. Maki et al. (1995) found that in cultured hippocampal neurons, the frequency-dependent depression of excitatory synaptic transmission is independent of activation of presynaptic mGluRs that are sensitive to (RS)- α -methyl-4-carboxyphenylglycine. Similarly, Silver et al. (1998) found that mGluRs do not affect STD in the synapses that climbing fibres make on Purkinje cells. Consistent with these results, as indicated above (observation #5), Markram and Tsodyks (1996) reported that STD was not affected by the blockade of mGluRs with 2-amino-5-phosphonopropionic acid. Therefore, presynaptic inhibition by mGluRs is not modeled in this study.

Any decrease in presynaptic Ca^{2+} current has a direct effect on transmitter release. However, a significant decrease in this current may necessitate several episodes of prolonged presynaptic depolarization (Klein et al., 1980), which could be achieved by several bursts of high frequency spike trains consisting of tens of spikes. Decrease in presynaptic Ca^{2+} influx due to inactivation of presynaptic Ca^{2+} channels may not be significant after brief stimulations such as those of Markram and Tsodyks (1996) (Fox et al., 1987; Lemos and Nowycky, 1989; Cox and Dunlap, 1994; Forsythe et al., 1998; Patil et al., 1998; Wu et al., 1998). Consequently, the inactivation of presynaptic Ca^{2+} channels is not likely to significantly contribute to STD in the target experiments, and is not modeled in this study.

The Approximate Model. The models of vesicle depletion (Figure 2), AMPAR desensitization (Equations 8-13) and vesicle priming (Equations 14-16) are combined in a stochastic synapse model, which is an inhomogeneous Markov chain (Karlin and Taylor, 1975). This model is used to generate simulated EPSP trains and is capable of predicting the variability in the data. The usual techniques of parameter estimation that are used with hidden Markov models (Chung et al., 1990) are intractable when directly used for an inhomogeneous Markov chain of the complexity modeled herein, and other methods must be used. The model parameters that yield the best fit to the target data may be found by fitting the average of a number of simulated EPSP trains to the data in Figure 1b and by

varying the model parameters until the fit error is minimized. As this method necessitates the averaging of a number of simulated EPSP traces for each candidate parameter configuration, it is computationally expensive. The search time would be drastically reduced if the average behavior of the stochastic model could be modeled by an *approximate* deterministic model.

Here it is proposed that the average behavior of the stochastic model may be captured by such a deterministic approximate model. This model is obtained by exploiting the fact that the release sites in the stochastic model are identical to each other in their average behavior. Also, some of the model variables (e.g. $R_{n,c}$ and $S_{n,c}$ in Equations 8-11) that are statistically dependent are treated as independent to make the computations tractable. Simulations show that the output of the approximate model is surprisingly close to the average behavior of the actual stochastic model (Figure 3).

Figure 3 shows the fit error predicted by the approximate model (dashed line) and the actual stochastic model (solid lines) as the parameter ε was varied while all other parameters were fixed at their optimal values, which were found by fitting the approximate model to the data. The lower solid line was obtained by computing the difference between the post-pairing data and the average of 10^5 simulated traces, which essentially represents the true average behavior of the stochastic model. The upper solid line was obtained by computing the average difference between the post-pairing data and the average of 59 simulated traces, as the post-pairing data were obtained as the average of 59 traces in Figure 1b. As expected, the minimum of both solid curves occurs at the same parameter value. It can be shown that the average error computed based on the average of 59 simulated traces is larger than that based on 10^5 traces because the EPSPs computed as the average of 59 traces have a larger variance. For the purpose of finding the optimal parameters, however, the only important question is whether the fit errors predicted by the approximate and the stochastic models are minimized at the same parameter value. Figure 3 shows that these minima indeed occur at nearly identical values of ε . Thus the optimal parameters found by the approximate model will also be optimal for the stochastic model in fitting the data of Figure 1b under original experimental conditions, i.e. for $M=58$ or 59. Therefore the search for the optimal parameter values is conducted using the approximate model, which reduces the computation time approximately a few thousand-fold, as the average of a few thousand simulated traces must be computed to obtain statistically significant comparisons between candidate parameter sets. Equations 17-26 represent the approximate model (See Appendix for derivations):

$$E_n = ACR_n S_n, \quad (17)$$

$$X_{n+1} = [X_n \varepsilon \rho_n + 1 - p_n] \pi G + X_n [\varepsilon(1 - \rho_n) + (1 - \varepsilon)] \Phi + (p_n - X_n) \pi (1 - \gamma), \quad (18)$$

$$p_{n+1} = 1 - \alpha + \alpha p_n \left(1 - \frac{X_n \varepsilon \rho_n}{p_n} \right), \quad (19)$$

$$S_n = 1 - x_n - y_n, \quad (20)$$

$$x_{n+1} = \lambda_1 (x_n + A_1 S_n R_n), \quad (21)$$

$$y_{n+1} = \lambda_2 (y_n + A_2 S_n R_n), \quad (22)$$

where E_n approximates the average EPSP amplitude elicited by the n^{th} AP, A is the absolute synaptic efficacy, which is the maximal EPSP amplitude that can be elicited per contact, C denotes the number of synaptic contacts per connection, R_n approximates the average transmitter output seen by the postsynaptic terminal and is a function of X_n , X_n approximates the probability that a primed vesicle is found at a given release site in an active zone, ρ_n approximates the probability that a primed and selected vesicle undergoes release, p_n approximates the probability that a vesicle is found at a given release site in an

active zone, S_n approximates the average postsynaptic sensitivity of a contact at the time of the n^{th} AP, $\lambda_1 = \exp(-\Delta t/0.056)$, and $\lambda_2 = \exp(-\Delta t/0.767)$. The expressions for R_n and ρ_n depend on the release mode. In the multivesicular release mode:

$$R_n = 1 - (1 - \omega X_n \varepsilon)^N, \quad (23)$$

$$\rho_n = 1, \quad (24)$$

and in the univesicular mode:

$$R_n = \omega \left[1 - (1 - X_n \varepsilon)^N \right], \quad (25)$$

$$\rho_n = \frac{1 - (1 - X_n \varepsilon)^N}{NX_n \varepsilon}. \quad (26)$$

Note that the exocytotic probability $u_{n,r,c}$ in Figure 2 corresponds here to the probability $X_n \varepsilon$, where the indexes r and c are dropped due to the symmetry among different sites. G and Φ are used from Equations 15-16.

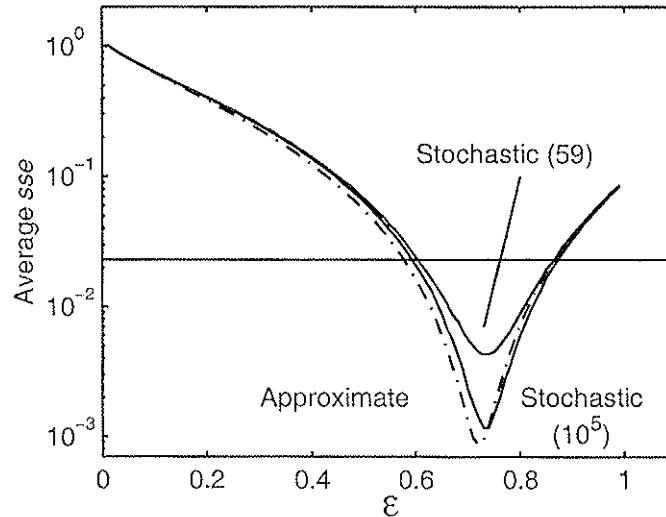


Figure 3. Comparison of the average fit error predicted by the deterministic approximate model and the actual stochastic model. All model parameters, except for ε (the primed vesicle selection probability), were fixed at the optimal values that were found by using the approximate model and that minimized the fit error to both the pre- and post-pairing data simultaneously (See Results associated with Figure 7). The average

sum-squared-error is given by $E(sse) = E\left(\sum_{n=1}^7 (E_n - d_n)^2\right)$, where E_n is the simulated average EPSP

amplitude obtained using the approximate or the stochastic model, and d_n is the post-pairing EPSP amplitude measured from Figure 1b. Dashed line: average sse obtained by using the approximate model (Equations 17-26 below). Since the approximate model is deterministic, taking the average value of sse is immaterial in this case as E_n is not a random variable. Solid lines: average sse obtained by using the stochastic model as follows. Average EPSP amplitudes $EPSP_{n,M}$ were computed using the actual stochastic model, where M denotes the number of simulated traces that were averaged. Note that $EPSP_{n,M}$ is a random variable. For the upper solid curve $E_n = EPSP_{n,59}$, and for the lower solid curve $E_n = EPSP_{n,100,000}$. The latter essentially represents the true average behavior of the stochastic model ($EPSP_{n,\infty}$), and is close to the dashed line, which approximates $EPSP_{n,\infty}$. The average sse based on $M=59$ is larger than that based on $M=10^5$ because the variance of $EPSP_{n,M}$ is larger for $M=59$ than for $M=10^5$. At the optimal parameter point, 97.59% of the sse generated using $M=59$ lied below the horizontal line. See Results for the use of this level. See Figure 7 for model parameter values (post-pairing).

The proposed loci of the model parameters and variables associated with depletion, priming, and exocytosis are shown in Figure 4. A synaptic contact that has $N=5$ release sites is shown. Except for the fourth site, each site has a docked vesicle. The vesicles at the first and the fifth sites are also primed. The fourth site, which was recently depleted, is being refilled with a time constant of $\tau_{\text{refill}}=0.2$ s. The parameters τ and π are computed from the forward and reverse reaction rates of priming (Equation 14). The primed vesicle selection probability ε depends on the sensitivity of the Ca^{2+} sensor of the release machinery, and the intensity of the Ca^{2+} influx through the voltage-gated Ca^{2+} channels.

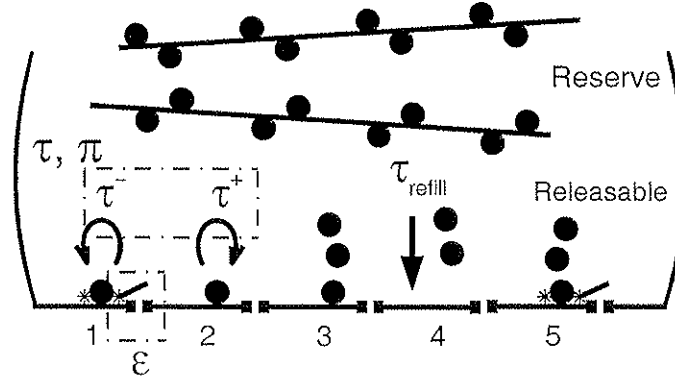


Figure 4. Illustration of the presynaptic terminal and the processes that are being modeled. In the reserve pool, the vesicles are anchored to actin filaments (black bars) via the membrane protein synapsin. It is assumed that this pool is not depleted during the brief stimulations shown in Figure 1. Vesicle depletion is significant only in a releasable vesicle pool of 2-3 vesicle layers. The synaptic contact (active zone) contains $N=5$ release sites. Inserted into the presynaptic membrane are voltage-gated Ca^{2+} channels. Docked and primed vesicles are shown at the first and fifth sites. The Ca^{2+} sensor of the release machinery is represented by the small line segment that extends toward the Ca^{2+} channel. An increase in the model parameter ε may represent an increase in either the sensitivity of the Ca^{2+} sensor or the intensity of the Ca^{2+} influx through the channel. The model parameters τ and π are computed using the forward ($1/\tau^+$) and reverse ($1/\tau^-$) reaction rates of priming (Equation 14). Vesicles that are docked but not yet primed are shown at the second and third sites. Their instantaneous rate of priming is $1/\tau^+$ at the present state. The refilling of a recently emptied release site is illustrated at the fourth site. The time constant of refilling is $\tau_{\text{refill}}=0.2$ s. Each such synaptic contact faces a postsynaptic side (not shown) whose sensitivity is represented by the variable S (Equations 20-22). In TL5-TL5 synapses $C=4-8$ synaptic contacts are found per synaptic connection.

The approximate model was used to search for the optimal model parameters A , C , ε , N , π , and τ , that minimized the sum-squared-error between the predicted average EPSP amplitudes and observed average EPSP amplitudes in Figure 1: The search was conducted under the constraints of $\tau^+ < 5$ s, $\text{Pr}_{\text{pre}} = 97.4 \pm 2.17\%$, $\text{Pr}_{\text{post}} = 99.67 \pm 0.25\%$ (Markram and Tsodyks, 1996), and $\text{c.v.} = 0.5 \pm 0.5$ (Markram et al., 1997), where Pr_{pre} and Pr_{post} refer to the probability of release at the first AP before and after pairing, respectively, and c.v. refers to the coefficient of variation of the first EPSP amplitude. All other model parameters were fixed at the values indicated earlier. C was changed from 4 to 8 with steps of 1, N from 1 to 25 with steps of 1, τ from 0.5 s to 1.5 s with steps of 50 ms, and the probabilities ε and π from 0.01 to 1 with steps of 0.01. The range for τ was chosen based on the observation that the overall time constant of recovery from STD in these synapses

was observed to lie in the indicated range (Markram, 1997). The curves in Figure 3 were computed after the optimal parameter values were found as just described.

Statistical Methods. In the target experiments (Figure 1), the average post-pairing EPSP amplitudes were computed as the average of 59 traces (Markram and Tsodyks, 1996). This method is also adopted in the simulations. Thus, in obtaining the results shown in Figures 5 and 6, the simulated paired-pulse-depression (PPD) ratio that was computed by using the stochastic model was the ratio of the second to the first EPSP amplitude in an average of 59 simulated traces. To compute the probability of observing a PPD value below 32.26% in Figures 5 and 6, the random variable Y is considered, where $Y=1$ if $PPD_i \leq 32.26\%$, and $Y=0$ otherwise, with PPD_i being a sample PPD generated by the model in the i^{th} experiment. The probability that the PPD generated in a simulated experiment is smaller than 32.26% is denoted by the constant " β " and depends on the model parameters. Thus, $\Pr(Y=1)=\text{mean}(Y)=\beta$. The value of β is estimated as follows: Simulated experiments are run to generate M samples of Y . Let M denote the number of times $Y=1$ is observed in these M trials. An estimate of β is computed as $b=M/M$. Using the Central Limit Theorem, the minimum number M of samples that are needed to have $|b-\beta|<k/100$ with at least $L\%$ confidence may be determined. Specifically: $L/100 \geq 2\Phi(0.02k\sqrt{M})-1$, where $\Phi(x)$ is the standard normal distribution function (Dudewicz and Mishra, 1988). Here, the inequality originates from the use of the upper bound of the variance of Y , i.e. 0.25, in place of the variance of Y ($\text{var}(Y)=\beta(1-\beta)\leq 0.25$). Note that the use of the Central Limit Theorem ordinarily depends on the exact variance of Y . The approach described above circumvents this parameter-dependence by substituting 0.25 in place of $\text{var}(Y)$. In Figures 5 and 6, $L=99$ and $k=1$, which yields $M=16,641$.

RESULTS

The Extent of Synaptic Depression that is Due to Vesicle Depletion

A synaptic model that consists only of the depletion of the releasable vesicle pool does not explain the strong STD observed in the post-pairing data. In Figure 1, the average EPSP amplitudes recorded after pairing indicate that the paired-pulse depression (PPD) ratio, which is the ratio of the second EPSP amplitude to the first, is about 32.26%. By preventing the depression that is due to components other than vesicle depletion, the stochastic model was used to simulate these experiments, and it was found that even for the parameter values that result in the strongest depression, a PPD ratio of 32.26% could not be obtained. The AMPAR desensitization was prevented by setting $A_1=A_2=0$. Priming was ensured by setting $\tau=0.1$ ms, and $\pi=1$. Under these conditions, the release probability at the first AP is given by:

$$\Pr = 1 - (1 - \varepsilon)^{NC}, \quad (27)$$

where \Pr is measured experimentally. Equation 27 can thus be used to determine the value of ε given N and C .

The strongest depression is obtained for the smallest numbers N of the release sites, and C of the synaptic contacts. Figure 5 illustrates the probability of observing a $PPD \leq 32.26\%$ in simulated experiments, for different choices of N and C , in the multivesicular mode. All probabilities are within 0.01 of the shown value (significance $P < 0.01$). Thus, all probabilities that are shown as zero were less than 1% ($P < 0.01$). In particular, for $N > 2$ no C value resulted in a probability $> 1\%$. The results were naturally the same in the univesicular mode for $N=1$. However, for $N > 1$ no C value resulted in a probability $> 1\%$ in the univesicular mode.

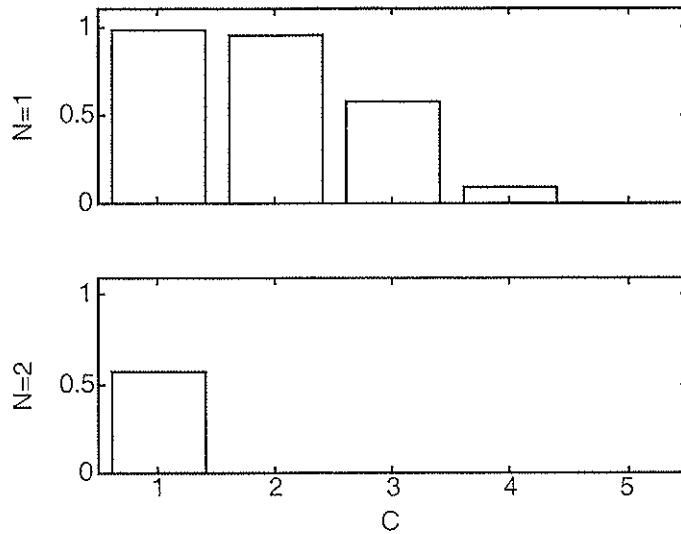


Figure 5. The probability of observing $PPD \leq 32.26\%$ in simulated experiments using vesicle depletion only. The experiment in Figure 1 was simulated as explained in the Methods, using the stochastic model that consisted only of the depletion of the releasable vesicle pool. The exocytotic probability ε was computed using Equation 27 with $Pr=99.67\%$ as reported by Markram and Tsodyks (1996). Shown are the probability that the simulated $PPD \leq 32.26\%$ in multivesicular mode. The simulated PPD was within 1% of the shown values, with significance $P < 0.01$. Probabilities for $N > 2$ or $C > 5$ were less than 1% ($P < 0.01$). In univesicular mode the probabilities for $N=1$ were as shown, but for $N > 1$ all probabilities were less than 1% ($P < 0.01$).

The results show that vesicle depletion alone may not explain the strong STD observed experimentally, unless one assumes that there can only be $N=1$ release site per active zone in univesicular mode with less than $C=4$ functional synaptic contacts per synaptic connection despite the fact that these synapses have 4 to 8 synaptic contacts (Markram et al., 1997). Similarly, if the release is multivesicular, no more than 2 release sites must be present per active zone, and there must be only one functional synaptic contact in order for the depletion to result in a PPD close to 32.26% for $N=2$. These conditions are not met in the TL5-TL5 synapses, however, since the physiological and anatomical estimates of the functional contacts in TL5-TL5 synapses appear consistent, implying that C must be between 4 and 8 (Henry Markram, personal communication, February 3, 2001). Even if the synapse under study had silent contacts and had no more than 2 release sites per its functional active zones, these predictions suggest that a large group of synapses that have at least 4 functional synaptic contacts may not exhibit such a strong depression. Also, if silent synapses do exist in TL5-TL5 synapses, and they behave like the hippocampal silent synapses that become activated after potentiation (Isaac et al., 1995; Liao et al., 1995), then it would be expected that 4 functional synaptic contacts is not uncommon for synapses potentiated by Hebbian pairing. Recalling that the observed PPD of 32.26% arose after pairing, we infer that vesicle depletion alone is unlikely to account for the strong short-term depression observed after Hebbian pairing in Figure 1. Using a similar analysis, Matveev and Wang (2000) also concluded that vesicle depletion alone cannot yield the strong STD observed in depressing cortical synapses. Additional synaptic processes that contribute to STD must therefore be incorporated into the stochastic model. Next treated is whether a model including AMPAR desensitization as an additional depressing process is still insufficient to explain the strong STD observed in the post-pairing data.

The Extent of Synaptic Depression that is Due to Vesicle Depletion and AMPAR Desensitization

The AMPAR desensitization may be reactivated by setting $A_1=0.18$ $A_2=0.30$, while the depression due to priming is still prevented. The resulting model is still unable to explain the observed level of STD.

As in the previous section, the model may be used to compute the probability of observing $PPD \leq 32.26\%$. Figure 6 shows that this probability is not high if $C \geq 4$ or $N > 3$. Although the inclusion of AMPAR desensitization increased the synaptic depression, this increase was not large enough. In summary, the combined effects of vesicle depletion and AMPAR desensitization may not explain the strong STD observed experimentally. These results suggest that an additional synaptic process that contributes to STD must be incorporated into the stochastic model. The next section presents the results that were obtained when the additional depression that is due to priming was not prevented.

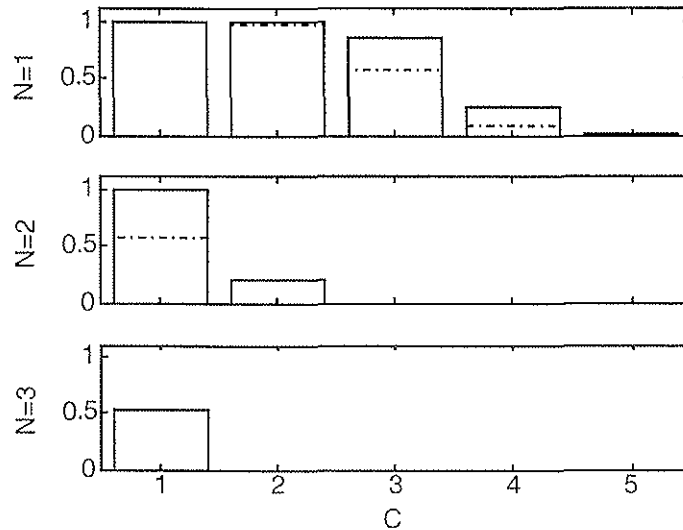


Figure 6. The probability of observing $PPD \leq 32.26\%$ in simulated experiments using vesicle depletion and AMPAR desensitization only. The experiment in Figure 1 was simulated using the stochastic model that consisted only of the depletion of the releasable vesicle pool and AMPAR desensitization. Dashed lines: The results shown in Figure 5 (Depletion only). Solid lines: Depletion and AMPAR desensitization. The exocytotic probability ε was computed using Equation 27 with $Pr=99.67\%$ as reported by Markram and Tsodyks (1996). Shown are the probability that the simulated $PPD \leq 32.26\%$ in multivesicular mode. The probabilities were within 1% of the shown values, with significance $P < 0.01$. Probabilities for $N > 3$ or $C > 5$ were less than 1% ($P < 0.01$). In univesicular mode the probabilities for $N=1$ were as shown, but for $N > 1$ all probabilities were less than 1% ($P < 0.01$).

A Stochastic Priming Process Explains Strong Short-term Depression

As noted, a vesicle that arrives at a release site is thought to undergo a priming process whereby it is attached to the presynaptic membrane by a specialized protein complex. The formation of this complex is a reversible reaction, with reaction time constants on the order of a few seconds (Chow et al., 1994; Heinemann et al., 1994; Banerjee et al., 1996; Otto et al., 1997; Ungermann et al., 1998; He et al., 1999; Xu et al., 1999). Because of the reversibility of the primed state, the probability of finding a primed vesicle at a release site is smaller than 1, even following a long rest period. This renders only a few of the docked vesicles eligible for release at a given time. Moreover, if a docked vesicle is not found in the primed state at an observation time $t=0$, then the probability of finding it in the primed state at a later time t is given by Equation 14, which suggests that priming acts like a depressing process that recovers slowly. These observations suggest that the inclusion of

the priming in the model could result in sufficient depression to explain the strong STD observed in the target data.

By enabling priming, the full approximate model with vesicle depletion, AMPAR desensitization and priming was used to search for the optimal model parameters that minimized the sum-squared-error from the data in Figure 1b. In this search, some of the variable model parameters were constrained to have the same value before and after pairing. These parameters were N , C , τ , and π . Of these parameters, τ was constrained because it is experimentally observed that the overall time constant of recovery from STD is not changed by Hebbian pairing (Markram and Tsodyks, 1996). Note that τ is obtained from the reaction rates of priming (Equation 14), and thus Hebbian pairing appears not to affect the priming reaction rates. As the parameter π also depends on these reaction rates, π is constrained as well. In addition, the time constant τ^+ of the forward priming reaction was constrained to be less than 5 s. The number C of synaptic contacts is constrained based on the observation that the physiological and anatomical estimates of this number appear to agree, which argues against the presence of silent synapses (Henry Markram, personal communication, February 3, 2001). Although this number could change in time in an activity-dependent way, the fact that the post-pairing data were collected 20 min after pairing suggests that a structural change of this type might not have happened in this time frame. Similarly, the number N of release sites per active zone may not have changed. In addition to these, the probability of release at the first AP was constrained to be higher in the post-pairing case than in the pre-pairing case (Markram and Tsodyks, 1996; Tsodyks and Markram, 1997), and the coefficient of variation of the first EPSP amplitude was constrained to be smaller in the post-pairing case.

The approximate model was used under the above constraints to search for the optimal parameters. These parameters were then used to simulate the experiments associated with Figure 1 using the stochastic model. Figure 7 shows the results of these simulations.

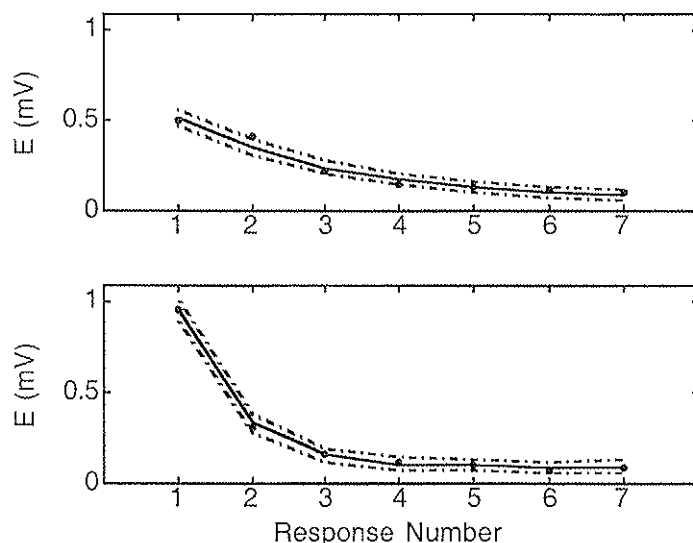


Figure 7. Fits generated by the stochastic model using the optimal parameters found by the approximate model. Solid circles represent the data points taken from Figure 1b. The solid line shows the average model output. The dashed lines represent the 95% confidence interval for the average of 59 simulated traces. $N=13$, $C=4$, $\tau=0.6$ s, $\pi=0.17$ in both cases. Before pairing (upper plot): univesicular mode, $A=0.3166$ mV, $\varepsilon=0.5$. After pairing (lower plot): multivesicular mode, $A=0.3841$ mV, $\varepsilon=0.72$.

The fit to the post-pairing data shows that the inclusion of priming into the model indeed resulted in sufficient depression to explain the strong PPD observed in the data.

The Predicted Effect of Hebbian Pairing

The difference between the optimal parameters for the pre- and post-pairing cases constitutes the model's prediction for the effects of Hebbian pairing. The model predicts that there is not a large change in the maximal EPSP amplitude A elicited per contact, while a large change occurs in the probability ε that a primed vesicle undergoes release in response to an AP (Figure 7 legend). The results also show that the pre-pairing data are fitted better in the univesicular mode, while the post-pairing data are fitted better in the multivesicular mode. The increase in ε may be due to an increased AP-induced Ca^{2+} influx through voltage-gated presynaptic Ca^{2+} channels, or to an increased sensitivity of primed vesicles to this influx (Figure 4). The fact that pairing does not affect the rate of recovery from STD suggests that, in the latter scenario, the increase in the sensitivity of the primed vesicles to calcium must be expressed in a way that does not affect the rate of priming reactions.

The conclusions that are drawn by comparing the optimal parameter sets were verified by comparing parameter sets that perform comparably to the optimal. An analysis was conducted to determine a set of parameters that perform comparably to the optimal parameters, and the pairing-induced changes in those parameters were noted. These parameters were determined as follows. The experiments associated with Figure 1 were simulated using the stochastic model with the optimal parameters used in Figure 7. Each simulated experiment yielded a sum-squared-error (sse) that was obtained from the difference between the average model output and the data. The simulated experiment was repeated enough times to estimate the 97.5 ± 1 th percentile ($sse_{97.5}$) of the error distribution with a 95% confidence level. This level is indicated by the horizontal bar in Figure 3. Then, the approximate model was used to search the entire parameter space to find all parameters that resulted in a sse that was smaller than $sse_{97.5}$, subject to the search constraints discussed previously. This method provided a fast way of determining a set of parameters that perform comparably to the optimal parameters. The distribution of values in this set was then obtained for each parameter.

This analysis showed that 67% of the 2,096,536 pre-pairing parameters predicted the univesicular mode, and 100% of the same number of post-pairing parameters predicted the multivesicular release mode, suggesting that the pre-pairing data were slightly better fitted in the univesicular release mode. Also, the value of the parameter A was observed to take on values between 0.24-0.45 mV before pairing, and 0.28-0.51 mV after pairing, indicating no large change in the value of this parameter. However, ε was observed to take on values between 0.25-0.79 before pairing, and 0.51-0.9 after pairing, indicating a large change in the value of this parameter. All these results are consistent with the conclusions drawn from the optimal parameters. Another result of this analysis was to obtain the range of values taken by the parameters that were constrained not to change in pre- and post-pairing cases. Thus the values taken by these parameters were: N : 1-25, π : 0.1-1, C : 4-8, and τ : 0.5-1.5 s. Because these represent the entire ranges of experimentally observed values for N , C and τ , these results suggest that the data in Figure 1 could be obtained from virtually any synapse simply by increasing the post-priming exocytotic probability ε after pairing.

DISCUSSION

The present study proposes that the strong STD observed in some cortical synapses may be explained in terms of a slow priming process. Vesicle priming constitutes a rate-limiting step in synaptic transmission (Südhof, 1995) and the associated reaction time constants of a few seconds are in the appropriate order of magnitude to explain the rate of recovery from STD in the target experiments (Chow et al., 1994; Heinemann et al., 1994). It is shown that a stochastic synapse model that incorporates the processes of the depletion of the releasable vesicle pool, postsynaptic AMPAR desensitization, and vesicle priming is able to explain data on both STD and plasticity induced by Hebbian pairing.

STD has previously been linked to vesicle depletion (Liley and North, 1953; Grossberg, 1969; Betz, 1970; Zucker, 1989; Senn et al., 2001), postsynaptic AMPAR desensitization (Trussell et al., 1993; Jones and Westbrook, 1996; Tsodyks and Markram, 1996), and calcium-induced inactivation of release machinery (Hsu et al., 1996; Bellingham and Walmsley, 1999; Matveev and Wang, 2000). It is argued, in this study, that the depletion of the releasable vesicle pool will not by itself explain the experimentally observed levels of STD. Specifically, under the conditions of univesicular release, the presence of more than one releasable vesicle per active zone makes it impossible to obtain a PPD ratio that is smaller than 50% (Matveev and Wang, 2000). On the other hand, in the multivesicular release mode, the required level of STD is not obtained because the release probability per synaptic contact is not high enough to cause significant vesicle depletion. Note that the presence of more than one synaptic contact per synaptic connection may result in a very high release probability per connection, as high as 0.9967 (Markram and Tsodyks, 1996), while the release probability per synaptic contact is as low as 0.51 ($C=8$). These results are summarized in Figure 5 using the present stochastic model.

STD may also be partly explained in terms of the desensitization of postsynaptic transmitter receptors (Tsodyks and Markram, 1996). Here a double-exponential model of AMPAR desensitization is used, in keeping with the results of Jonas et al. (1994) that showed that the recovery from desensitization proceeds with two time constants in layer 5 pyramidal synapses. Although the inclusion of AMPAR desensitization resulted in more depression in simulations, Figure 6 shows that depletion and desensitization were not sufficient to explain the data. The reason why receptor desensitization does not contribute much to STD despite a slow recovery time constant is that its occurrence is conditional upon the occurrence of transmitter release. With a low release probability per synaptic contact, the postsynaptic side of each contact is not frequently exposed to transmitter release and thus does not experience desensitization frequently enough to sustain a large level of desensitization.

The insufficiency of vesicle depletion in explaining STD was noted earlier by Matveev and Wang (2000). This was also noted by Bellingham and Walmsley (1999), who also pointed out that the depression beyond vesicle depletion was not completely explained by AMPAR desensitization either. Both studies proposed that the residual depression may be due to calcium-induced inactivation of release machinery (IRM) (Hsu et al. 1996). For the experiments in Figure 1, however, IRM may not be applicable in explaining the observed STD for two reasons. First, the recovery from the depression that was attributed to IRM proceeded with a time constant of about 10 ms in the studies of Bellingham and Walmsley (1999). This is too fast to explain the present data. Second, the STD observed in pyramid-pyramid synapses in the neocortex is predominantly release-dependent (Thomson and Bannister, 1999). Namely, STD is not observed unless transmitter release occurs. In explaining the cortical STD data, however, Matveev and Wang (2000) implemented a release-independent IRM. In other words, each presynaptic AP inactivated the release machinery regardless of whether transmitter release occurred from the presynaptic terminal. Although STD is predominantly release-dependent in cortical pyramid-pyramid synapses, some release-independent depressing process that recovers with a time constant of less than about 10 ms is sometimes observed in these synapses (Alex Thomson, personal

communication, October 12, 2000). The fact that this time constant agrees with that observed by Bellingham and Walmsley (1999) suggests that this release-independent depressing process might correspond to IRM, if the latter exists in the cortical pyramid-pyramid synapses. Because of these difficulties, it is concluded here that IRM does not appear to be the mechanism that is responsible for explaining the target data.

The additional depression required to explain the data in Figure 1 is proposed here to be due to vesicle priming. Vesicle priming is implemented as a reversible process with reaction time constants comparable to those reported in other systems. The results show that priming not only explains the strong depression observed in the data, but also allows this depression to occur in a release-dependent fashion, which is consistent with the results of Thomson and Bannister (1999). Moreover, the parameters associated with the priming process, which are estimated by the model, suggest that priming is also consistent with the observation that at most one vesicle may be released per synaptic contact per presynaptic AP (Redman, 1990; Korn and Faber, 1991; Stevens and Wang, 1995; Dobrunz and Stevens, 1997). The all-or-none release may be due to some winner-take-all process that allows only one of the fusion-competent vesicles to be released by preventing the release of the others (Schikorski and Stevens, 1997). This is the method used in the present model in the univesicular mode. However, the present results suggest that all-or-none release may be closely approximated even in multivesicular release mode, if the probability of finding a primed vesicle in a synaptic contact is low enough. For example, even though the optimal parameters predict the presence of $N=13$ release sites per synaptic contact in Figure 7, the probability π of finding a primed vesicle at steady-state being 0.17, the average number of primed vesicles per active zone is $13 \times 0.17 = 2.21$ at rest. Moreover, since each primed vesicle has a probability $\varepsilon=0.5$ of undergoing release in response to an AP, the model predicts the release of 1.105 vesicles per AP per synaptic contact on the average before pairing. As discussed above, fits comparable to those in Figure 7 were obtained by using a wide variety of synaptic parameters, which suggests that a model that predicts an even lower figure might still generate a fit comparable to the optimal. Thus, priming not only explains a release-dependent strong depression that fits the cortical data, but also provides a possible explanation of how an average of about one vesicle may be released per synaptic contact per AP, despite the fact that there may be up to two dozen docked vesicles per synaptic contact (Schikorski and Stevens, 1997).

The Predicted Effect of Hebbian Pairing

Hebbian pairing alters the properties of STD in cortical pyramidal synapses (Markram and Tsodyks, 1996; Tsodyks and Markram, 1997; Buonomano, 1999). The present results suggest that the effect of pairing is to increase the probability that a primed vesicle is released in response to an AP. The increase in presynaptic release probability is one possible mechanism by which potentiation is expressed in some synapses (Liley and North, 1953; Tsodyks and Markram, 1997; Senn et al., 2001). The results of the present study are consistent with these proposals, and suggest that the increase in release probability is due either to an increased AP-induced Ca^{2+} influx into the presynaptic terminal, or to an increased sensitivity of primed vesicles to this influx (Figure 4). Since pairing does not affect the rate of recovery from STD, the plasticity in the latter scenario appears to occur without affecting the rates of priming reactions.

Another prediction of the model has been that pairing might alter the release mode from univesicular to multivesicular. This prediction is not very strong however, because 33% of the parameters that performed comparably to the optimal predicted a multivesicular release mode before pairing. Thus, the results are also consistent with multivesicular release mode being the release mode both before and after pairing. As noted above, due to smaller release probability before pairing, the average number of vesicles that are released per synaptic contact per AP may be around one even though there may be several docked vesicles per contact. This may be observed as the occurrence of univesicular release in

experiments. After pairing, this average number may increase due to increased release probability, which would be consistent with the observation that multivesicular release is more likely to be observed under conditions of increased release probability (Tong and Jahr, 1994). Other evidence also suggests the presence of multivesicular release in central synapses, possibly including the TL5-TL5 synapses (Auger et al., 1998; Liu et al., 1999). Thus the present results are in agreement with the experimental observations that suggest the existence of multivesicular release in the synapses under study.

In conclusion, our results suggest that vesicle priming and subsequent exocytotic processes may explain the strong STD, and its interaction with LTP, in the cortical pyramid-pyramid synapses.

APPENDIX

The approximate model equations are derived by treating the stochastic model variables as representing their average values, and ignoring the statistical dependence between different variables. At the time of the n^{th} AP, a vesicle at a release site in a given active zone (synaptic contact) can be found in one of 5 different states. These states and related exocytotic events are listed in Table A.1 and are used in the derivation of the approximate model.

Table A.1 States of a release site, and their occurrence probability

State	Description	Probability	X_{n+1}	p_{n+1}
1	Primed, selected, released	$X_n \varepsilon \rho_n$	πG	$1 - \alpha$
2	Primed, selected, another site released	$X_n \varepsilon (1 - \rho_n)$	Φ	1
3	Primed, not selected	$X_n (1 - \varepsilon)$	Φ	1
4	Present, not primed	$p_n - X_n$	$\pi(1 - \gamma)$	1
5	Not present	$1 - p_n$	πG	$1 - \alpha$

A given release site in an active zone (synaptic contact) may be found at one of the five indicated states at the n^{th} AP. The second column explains the states and the third shows the probability of occurrence of a state. The fourth and fifth columns show the values of X and p at the next AP, given the indicated state at the present AP.

In Table A.1 the probability of each state and the associated event is indicated in the third column. The values of X and p at the next AP, conditioned on the indicated states, are given in columns 4-5. Note that release from a site occurs only if the site is in the first state.

The presence of a vesicle, its state of priming and being selected are all represented by binary flags in the stochastic model. At each AP, the value of these flags (0 or 1) are determined by generating a uniformly distributed random variable z that is compared to p_n , X_n , and ε , to determine the flag values. Note that the flag for the priming status cannot be 1 (primed) if a vesicle is absent (presence flag=0), thus the state of priming is conditional on the presence of a vesicle. Similarly, the flags for the state of selection is conditional on priming. All selected sites have equal probability ρ_n of undergoing release.

In the multivesicular mode, the probability $\rho_n = 1$, since all selected vesicles are released. This also implies that the state 2 does not apply to the multivesicular mode. In the univesicular mode, the probability ρ_n is given by Equation 26, which is derived as follows.

The probability $\rho_{n,j}$ that a selected vesicle is released is $1/(j+1)$ if j additional vesicles are selected in the same active zone. Summing these probabilities, we have:

$$\rho_n = \sum_{j=0}^{N-1} \rho_{n,j} \Pr(j) = \sum_{j=0}^{N-1} \frac{1}{j+1} \binom{N-1}{j} (X_n \varepsilon)^j (1 - X_n \varepsilon)^{N-1-j}, \quad (\text{A1})$$

$$\rho_n = \frac{1}{N} \sum_{j=0}^{N-1} \binom{N}{j+1} (X_n \varepsilon)^j (1 - X_n \varepsilon)^{N-1-j}, \quad (\text{A2})$$

$$\rho_n = \frac{1}{N X_n \varepsilon} \sum_{k=1}^N \binom{N}{k} (X_n \varepsilon)^k (1 - X_n \varepsilon)^{N-k}, \text{ with } k = j+1. \quad (\text{A3})$$

The Equation 26 is equal to A3 as the summation in A3 yields $1 - (1 - X_n \varepsilon)^N$.

The probability of finding a primed vesicle (X_{n+1}), and the probability of finding a vesicle (p_{n+1}) at the $n+1^{\text{st}}$ AP are computed by summing the products of the indicated values with the associated probabilities shown in Table A.1. Equations 18-19 are obtained by algebraic manipulations of these sums. Of the remaining model equations, that for E_n (Equation 17) is obtained by assuming that the EPSP amplitude is proportional to the product of the average presynaptic output seen by the postsynaptic terminal at the n^{th} AP (R_n) and the average postsynaptic sensitivity at that AP (S_n). Since each contact acts independent of the other contacts, the average EPSP elicited per connection is C times that elicited per contact.

The computation of S_n is as in Equations 8-10. The approximate expression of R_n is computed from Equation 11. In the univesicular mode, the presynaptic output seen by the postsynaptic terminal is zero if no release occurs, and ω , which is the fraction of receptors occupied by the transmitter content of a single vesicle, if any of the sites in a contact releases. Release occurs with probability $[1-(1-X_n\epsilon)^N]$, which is the factor multiplying ω in Equation 25. In the multivesicular mode, the presynaptic output varies according to Equation 2 as a function of the number of vesicles that are released. By weighing every possible output with its probability, and summing the resulting products, the expression in Equation 23 is obtained (Matveev and Wang, 2000).

REFERENCES

- Angulo MC, Lambolez B, Audinat E, Hestrin S, Rossier J (1997) Subunit composition, kinetic, and permeation properties of AMPA receptors in single neocortical nonpyramidal cells. *J Neurosci* 17:6685-6696.
- Auger C, Kondo S, Marty A (1998) Multivesicular release at single functional synaptic sites in cerebellar Stellate and Basket cells. *J Neurosci* 18:4532-4547.
- Banerjee A, Barry VA, DasGupta BR, Martin TFJ (1996) N-ethylmaleimide-sensitive factor acts at a prefusion ATP-dependent step in Ca^{2+} -activated exocytosis. *J Biol Chem* 271:20223-20226.
- Bellingham MC, Walmsley B (1999) A novel presynaptic inhibitory mechanism underlies paired pulse depression at a fast central synapse. *Neuron* 23:159-170.
- Benfenati F, Onofri F, Giovedi S (1999) Protein-protein interactions and protein modules in the control of neurotransmitter release. *Philos Trans R Soc Lond B Biol* 354:243-257.
- Betz WJ (1970) Depression of transmitter release at the neuromuscular junction of the frog. *J Physiol* 206:629-644.
- Bittner MA, Holz RW (1992) Kinetic analysis of secretion from permeabilized adrenal chromaffin cells reveals distinct components. *J Biol Chem* 267:16219-16225.
- Bliss TVP, Lømo T (1973) Long-lasting potentiation of synaptic transmission in the dentate area of the anaesthetized rabbit following stimulation of the perforant path. *J Physiol* 232:331-356.
- Brodin L, Löw P, Gad H, Gustafsson J, Pieribone VA, Shupliakov O (1997) Sustained Neurotransmitter Release: New Molecular Clues. *Eur J Neurosci* 9:2503-2511.
- Buonomano DV (1999) Distinct functional types of associative long-term potentiation in neocortical and hippocampal pyramidal neurons. *J Neurosci* 19:6748-6754.
- Castillo PE, Janz R, Südhof TC, Tzounopoulos T, Malenka RC, Nicoll RA (1997) Rab3A is essential for mossy fibre long-term potentiation in the hippocampus. *Nature* 388:590-593.
- Chow RH, Klingauf J, Neher E (1994) Time course of Ca^{2+} concentration triggering exocytosis in neuroendocrine cells. *Proc Natl Acad Sci U S A* 91:12765-12769.
- Chung SH, Moore JB, Lige X, Premkumar S, Gage PW (1990) Characterization of single channel currents using digital signal processing techniques based on Hidden Markov Models. *Philos Trans R Soc Lond B Biol* 329:265-285.
- Colquhoun D, Jonas P, Sakmann B (1992) Action of brief pulses of glutamate on AMPA/KAINATE receptors in patches from different neurones of rat hippocampal slices. *J Physiol* 458:261-287.
- Cox DH, Dunlap K (1994) Inactivation of N-type calcium current in chick sensory neurons: calcium and voltage dependence. *J Gen Physiol* 104:311-336.
- Diamond JS, Jahr CE (1995) Asynchronous release of synaptic vesicles determines the time course of the AMPA receptor-mediated EPSC. *Neuron* 15:1097-1107.
- Dobrunz LE, Stevens CF (1997) Heterogeneity of release probability, facilitation, and depletion at central synapses. *Neuron* 18:995-1008.
- Doussau F, Clabecq A, Henry J, Darchen F, Poulain B (1998) Calcium-dependent regulation of Rab3 in short-term plasticity. *J Neurosci* 18:3147-3157.
- Dudewicz EJ, Mishra SN (1988) Modern mathematical statistics. John Wiley & Sons.
- Eccles JC (1957) The physiology of nerve cells. Baltimore, MD: The Johns Hopkins Press.
- Elhamdani A, Martin TFJ, Kowalchuk JA, Artalejo CR (1999) Ca^{2+} -dependent activator protein for secretion is critical for the fusion of dense-core vesicles with the membrane in calf adrenal chromaffin cells. *J Neurosci* 19:7375-7383.
- Feng TP (1941) Studies on the neuromuscular junction. XXVI. The changes of the end-plate potential during and after prolonged stimulation. *Chin J Physiol* 16:341-372.

- Fox AP, Nowycky MC, Tsien RW (1987) Kinetic and pharmacological properties distinguishing three types of calcium currents in chick sensory neurons. *J Physiol (Lond)* 394:149-172.
- Forsythe ID, Tsujimoto T, Barnes-Davies M, Cuttle MF, Takahashi T (1998) Inactivation of presynaptic calcium current contributes to synaptic depression at a fast central synapse. *Neuron* 20:797-807.
- Forti L, Bossi M, Bergamaschi A, Villa A, Malgaroli A (1997) Loose-patch recordings of single quanta at individual hippocampal synapses. *Nature* 388:874-878.
- Geppert M, Goda Y, Stevens CF, Südhof TC (1997) The small GTP-binding protein Rab3A regulates a late step in synaptic vesicle fusion. *Nature* 387:810-814.
- Geppert M, Südhof TC (1998) Rab3 and synaptotagmin: the yin and yang of synaptic membrane fusion. *Annu Rev Neurosci* 21:75-95.
- Greengard P, Valtorta F, Czernik AJ, Benfenati F (1993) Synaptic vesicle phosphoproteins and regulation of synaptic function. *Science* 259:780-785.
- Grossberg S (1969) On the production and release of chemical transmitters and related topics in cellular control. *J Theor Biol* 22:325-364.
- He P, Southard RC, Chen D, Whiteheart SW, Cooper RL (1999) Role of α -SNAP in promoting efficient neurotransmission at the Crayfish neuromuscular junction. *J Neurophysiol* 82:3406-3416.
- Heinemann C, Chow RH, Neher E, Zucker RS (1994) Kinetics of the secretory response in bovine chromaffin cells following flash photolysis of caged Ca^{2+} . *Biophys J* 67:2546-2557.
- Hsu S, Augustine GJ, Jackson MB (1996) Adaptation of Ca^{2+} -triggered exocytosis in presynaptic terminals. *Neuron* 17:501-512.
- Isaac JTR, Nicoll RA, Malenka RC (1995) Evidence for silent synapses: implications for the expression of LTP. *Neuron* 15:427-434.
- Jahn R, Südhof TC (1999) Membrane fusion and exocytosis. *Annu Rev Biochem* 68:863-911.
- Jonas P, Major G, Sakmann B (1993) Quantal components of unitary EPSCs at the mossy fibre synapse on CA3 pyramidal cells of rat hippocampus. *J Physiol* 472:615-663.
- Jonas P, Racca C, Sakmann B, Seeburg PH, Monyer H (1994) Differences in Ca^{2+} permeability of AMPA-type glutamate receptor channels in neocortical neurons caused by differential GluR-B subunit expression. *Neuron* 12:1281-1289.
- Jones MV, Westbrook GL (1996) The impact of receptor desensitization on fast synaptic transmission. *Trends Neurosci* 19:96-101.
- Karlin S, Taylor HM (1975) A first course in stochastic processes. New York: Academic Press.
- Katz B (1969) The release of neural transmitter substances. Liverpool: Liverpool University Press.
- Klein M, Shapiro E, Kandel ER (1980) Synaptic plasticity and the modulation of the Ca^{2+} current. *J Exp Biol* 89:117-157.
- Korn H, Faber DS (1991) Quantal analysis and synaptic efficacy in the CNS. *Trends Neurosci* 14:439-445.
- Kriebel ME, Gross CE (1974) Multimodal distribution of frog miniature endplate potentials in adult, denervated, and tadpole leg muscle. *J Gen Physiol* 64:85-103.
- Lemos JR, Nowycky MC (1989) Two types of calcium channels coexist in peptide-releasing vertebrate nerve terminals. *Neuron* 2:1419-1426.
- Li L, Chin L, Shupliakov O, Brodin L, Sihra TS, Hvalby Ø, Jensen V, Zheng D, McNamara JO, Greengard P, Andersen P (1995) Impairment of synaptic vesicle clustering and of synaptic transmission, and increased seizure propensity, in synapsin I-deficient mice. *Proc Natl Acad Sci U S A* 92:9235-9239.

- Liao D, Hessler NA, Malinow R (1995) Activation of postsynaptically silent synapses during pairing-induced LTP in CA1 region of hippocampal slice. *Nature* 375:400-404.
- Liley AW, North KAK (1953) An electrical investigation of effects of repetitive stimulation on mammalian neuromuscular junction. *J Neurophysiol* 16:509-527.
- Lin RC, Scheller RH (2000) Mechanisms of synaptic vesicle exocytosis. *Annu Rev Cellular and Developmental Biol* 16:19-49.
- Liu G, Choi S, Tsien RW (1999) Variability of neurotransmitter concentration and nonsaturation of postsynaptic AMPA receptors at synapses in hippocampal cultures and slices. *Neuron* 22:395-409.
- Liu G, Tsien RW (1995) Properties of synaptic transmission at single hippocampal synaptic boutons. *Nature* 375:404-408.
- Magleby KL, Miller DC (1981) Is the quantum of transmitter release composed of subunits? A critical analysis in the mouse and frog. *J Physiol* 311:267-287.
- Maki R, Cummings DD, Dichter MA (1995) Frequency-dependent depression of excitatory synaptic transmission is independent of activation of MCPG-sensitive presynaptic metabotropic glutamate receptors in cultured hippocampal neurons. *J Neurophysiol* 74:1671-1674.
- Markram H (1997) A network of tufted layer 5 pyramidal neurons. *Cereb Cortex* 7:523-533.
- Markram H, Lübke J, Frotscher M, Roth A, Sakmann B (1997) Physiology and anatomy of synaptic connections between thick tufted pyramidal neurones in the developing rat neocortex. *J Physiol* 500:409-440.
- Markram H, Tsodyks M (1996) Redistribution of synaptic efficacy between neocortical pyramidal neurons. *Nature* 382:807-810.
- Markram H, Wang Y, Tsodyks M (1998) Differential signaling via the same axon of neocortical pyramidal neurons. *Proc Natl Acad Sci U S A* 95:5323-5328.
- Matveev V, Wang X (2000) Implications of all-or-none synaptic transmission and short-term depression beyond vesicle depletion: a computational study. *J Neurosci* 20:1575-1588.
- Neher E, Zucker RS (1993) Multiple calcium-dependent processes related to secretion in bovine chromaffin cells. *Neuron* 10:21-30.
- Otis T, Zhang S, Trussell LO (1996) Direct measurement of AMPA receptor desensitization induced by glutamatergic synaptic transmission. *J Neurosci* 16:7496-7504.
- Otto H, Hanson PI, Jahn R (1997) Assembly and disassembly of a ternary complex of synaptobrevin, syntaxin, and SNAP-25 in the membrane of synaptic vesicles. *Proc Natl Acad Sci U S A* 94:6197-6201.
- Patil PG, Brody DL, Yue DT (1998) Preferential closed-state inactivation of neuronal calcium channels. *Neuron* 20:1027-1038.
- Pieribone VA, Shupliakov O, Brodin L, Hilfiker-Rothenfluh S, Czernik AJ, Greengard P (1995) Distinct pools of synaptic vesicles in neurotransmitter release. *Nature* 375:493-497.
- Raman IM, Trussell LO (1995) The mechanism of α -amino-3-hydroxy-5-methyl-4-isoxazolepropionate receptor desensitization after removal of glutamate. *Biophys J* 68:137-146.
- Redman S (1990) Quantal analysis of synaptic potentials in neurons of the central nervous system. *Physiol Rev* 70:165-198.
- Rothman JE (1994) Mechanisms of intracellular protein transport. *Nature* 372:55-63.
- Scheller RH (1995) Membrane trafficking in the presynaptic nerve terminal. *Neuron* 14:893-897.
- Schikorski T, Stevens CF (1997) Quantitative ultrastructural analysis of hippocampal excitatory synapses. *J Neurosci* 14:5858-5867.

- Senn W, Markram H, Tsodyks M (2001) An algorithm for modifying neurotransmitter release probability based on pre- and post-synaptic spike timing. *Neural Comput* 13:35-67.
- Shao X, Li C, Fernandez I, Zhang X, Südhof TC, Rizo J (1997) Synaptotagmin-syntaxin interaction: the C2 domain as a Ca²⁺-dependent electrostatic switch. *Neuron* 18:133-142.
- Shupliakov O, Pieribone VA, Gad H, Brodin L (1996) Presynaptic mechanisms in central synaptic transmission: 'biochemistry' of an intact glutamatergic synapse. *Acta Physiol Scand* 157:369-379.
- Söllner T, Bennett MK, Whiteheart SW, Scheller RH, Rothman JE (1993a) A protein assembly-disassembly pathway in vitro that may correspond to sequential steps of synaptic vesicle docking, activation, and fusion. *Cell* 75:409-418.
- Söllner T, Whiteheart SW, Brunner M, Erdjument-Bromage H, Geromanos S, Tempst P, Rothman JE (1993b) SNAP receptors implicated in vesicle targeting and fusion. *Nature* 362:318-324.
- Stevens CF (1993) Quantal release of neurotransmitter and long-term potentiation. *Neuron* 10:55-63.
- Stevens CF, Tsujimoto T (1995) Estimates for the pool size of releasable quanta at a single central synapse and for the time required to refill the pool. *Proc Natl Acad Sci U S A* 92:846-849.
- Stevens CF, Wang Y (1995) Facilitation and depression at single central synapses. *Neuron* 14:795-802.
- Stevens CF, Wang Y (1994) Changes in reliability of synaptic function as a mechanism for plasticity. *Nature* 371:704-707.
- Ström G (1951) Physiological significance of post-tetanic potentiation of the spinal monosynaptic reflex. *Acta Physiol Scand* 24:61-83.
- Südhof TC (1995) The synaptic vesicle cycle: a cascade of protein-protein interactions. *Nature* 375:645-653.
- Thomson AM, Bannister AP (1999) Release-independent depression at pyramidal inputs onto specific cell targets: dual recordings in slices of rat cortex. *J Physiol* 519:57-70.
- Tong G, Jahr CE (1994) Multivesicular release from excitatory synapses of cultured hippocampal neurons. *Neuron* 12:51-59.
- Tong G, Shepherd D, Jahr CE (1995) Synaptic desensitization of NMDA receptors by calcineurin. *Science* 267:1510-1512.
- Trussell LO, Fischbach GD (1989) Glutamate receptor desensitization and its role in synaptic transmission. *Neuron* 3:209-218.
- Trussell LO, Zhang S, Raman IM (1993) Desensitization of AMPA receptors upon multiquantal neurotransmitter release. *Neuron* 10:1185-1196.
- Tsodyks MV, Markram H (1996) Plasticity of neocortical synapses enables transitions between rate and temporal coding. *Lecture Notes in Computer Science* 1112:445-450.
- Tsodyks M, Markram H (1997) The neural code between neocortical pyramidal neurons depends on neurotransmitter release probability. *Proc Natl Acad Sci U S A* 94:719-723.
- Turner KM, Burgoyne RD, Morgan A (1999) Protein phosphorylation and the regulation of synaptic membrane traffic. *Trends Neurosci* 22:459-464.
- Ungermann C, Nichols BJ, Pelham HRB, Wickner W (1998) A vacuolar v-t-SNARE complex, the predominant form in vivo and on isolated vacuoles, is disassembled and activated for docking and fusion. *J Cell Biol* 140:61-69.
- von Gersdorff H, Schneggenburger R, Weis S, Neher E (1997) Presynaptic depression at a calyx synapse: The small contribution of metabotropic glutamate receptors. *J Neurosci* 17:8137-8146.

- von Rüden L, Neher E (1993) A Ca-dependent early step in the release of catecholamines from adrenal chromaffin cells. *Science* 262:1061-1065.
- Wernig A, Stirner H (1977) Quantum amplitude distributions point to functional unity of the synaptic 'active zone'. *Nature* 269:820-822.
- Wu LG, Borst JG, Sakmann B (1998) R-type Ca^{2+} currents evoke transmitter release at a rat central synapse. *Proc Natl Acad Sci U S A* 95:4720-4725.
- Xu T, Ashery U, Burgoyne RD, Neher E (1999) Early requirement for α -SNAP and NSF in the secretory cascade in chromaffin cells. *European Molecular Biology Organization Journal* 18:3293-3304.
- Zucker RS (1989) Short-term synaptic plasticity. *Annu Rev Neurosci* 12:13-31.